The role of fat cells in treatment of ALS

Amyotrophic lateral sclerosis is a (heterogeneous) neurodegenerative disorder with a variable site of disease initiation and rate of progression. There are no established blood or CSF-based markers that outperform clinical observation to provide an early diagnosis, accurate prediction of disease progression, or clinical stratification of ALS phenotypic variants. Proinflammatory cytokines, reactive oxygen species, and pro-inflammatory lipid-derived compounds result in neuronal damage and supply a positive feedback loop of neuroinflammation. Pathways of inflammation have multiple and redundant initiation sites and that means that many proinflammatory cytokines can compensate in the absence of any single factor. Thus, it is unlikely that efforts to target a single factor in humans will provide significant therapeutic benefit in patients with ALS. It may be necessary to develop pluripotent treatments that can regulate multiple steps in inflammatory pathways.

Since many factors affect the onset and progression of ALS, it is important to identify biomarkers that aid the identification of drugs that influence and mitigate the damage. Targets are prevention of motor neuron loss and neuromuscular denervation. One approach to identifying biomarkers, as well as potential treatment targets, is by analyzing signals from adipose tissue cells (ATC's). The population of endothelial cells (supporting cells in fat tissue that contain stem cells) change over time and understanding how disease changes cell phenotype may be useful. If detrimental changes can be identified, patients can receive patient-specific treatments. An *in vitro* analysis of an individual's current disease state may direct treatment and is a worthy goal. Patient derived stem cells are active areas of investigation in ALS therapies and could provide useful treatment information.

Stem cells are used as a restorative therapy in ALS. The risk of damaging the nervous system and exacerbating disease with stem cells is apparent. In addition to physical damage, the transplanted cells are not homogenous across patients or appropriate at all stages of disease. Autologous (donated by the same person that is receiving them) stem cells are sensitive to their microenvironment. Consideration of the microenvironment is appropriate to both the source and destination of the transplanted cells.

Locally, motor neuron oxidative stress, as it occurs in ALS, is made worse by induction of uncoupling proteins. Uncoupling proteins disassociate specific energy (metabolic) pathways from mitochondria, often with harmful outcomes. Interestingly, in disease there is increased aerobic glycolysis, mitochondrial cell stress, low ATP and uncoupling protein upregulation that results in intracellular toxicity. In diabetes and mild obesity, there is an association with increased blood glucose that may be protective against ALS.

The pathogenesis of ALS may be due to a "crosstalk" between vascular endothelium in the central nervous system and cells in adipose (fat) tissue. Theoretically, as subclinical disease progresses to a clinical state, the crosstalk could signal and alter the adipose tissue. One possible effect is called "browning". Browning increases the beige/brown fat population, this fat produces heat at the expense of energy to the mitochondria. A local outcome of browning is an "uncoupling of ATP production from oxygen consumption in the electron transport chain. Mitochondrial uncoupling leads to futile cycling of ATP synthase, consuming oxygen, expending calories, and producing heat" (Yang 2017). We propose to evaluate ATC's from ALS patients for markers that would indicate browning.

When cells are cultured *in vitro* they secrete cytokines and growth factors, the media is called secretome. Paracrine secretions from stem cells found in some secretome benefit survival when tested in animal models of ALS. It is useful to study cell secretions provided in secretome/conditioned media

from *in vitro* culture of stem cells and their ability to modulate the immune and inflammatory pathways associated with ALS. It is possible that the secretome could effect a neuroprotective function for motor neurons. In this way, beneficial components associated with stem cells are administered to the patient once the correct consortium of agents are recognized. Stem cells are sourced from multiple tissues, ATC may prove uniquely beneficial.

Critical information to understand the application of stem cell secretome/conditioned media is adequately characterizing the effective components mediating therapeutic benefits and optimizing the medium for clinical application. A proposed source of conditioned media is from adipose stem cells, ASC. We anticipate that the diseased environment may influence the phenotype of ASC's and propose to evaluate the phenotype difference between normal and diseased donor derived ASC's.

The progress toward a stem cell based, cell-free therapy in humans has a precedent. The dysfunction and function of endothelial cells can be determined. Analysis of ASC's could provide a snapshot of an individuals disease and indicate an appropriate therapy.

TISSUE ENGINEERING: Part A
Volume 23, Numbers 7 and 8, 2017

DOI: 10.1089/ten.tea.2016.0399

termis
Tissue Engineering
& Regenerative Medicine
International Society

ORIGINAL ARTICLE

Metabolically Active Three-Dimensional Brown Adipose Tissue Engineered from White Adipose-Derived Stem Cells

Jessica P. Yang, MSE,[1,*] Amy E. Anderson, BS,[2,*] Annemarie McCartney, PhD,[2] Xavier Ory, MS,[3] Garret Ma, MSE,[1] Elisa Pappalardo, PhD,[4] Joel Bader, PhD,[4] and Jennifer H. Elisseeff, PhD[1]

Brown adipose tissue (BAT) has a unique capacity to expend calories by decoupling energy expenditure from ATP production, therefore BAT could realize therapeutic potential to treat metabolic diseases such as obesity and type 2 diabetes. Recent studies have investigated markers and function of native BAT, however, successful therapies will rely on methods that supplement the small existing pool of brown adipocytes in adult humans. In this study, we engineered BAT from both human and rat adipose precursors and determined whether these *ex vivo* constructs could mimic *in vivo* tissue form and metabolic function. Adipose-derived stem cells (ASCs) were isolated from several sources, human white adipose tissue (WAT), rat WAT, and rat BAT, then differentiated toward both white and brown adipogenic lineages in two-dimensional and three-dimensional (3D) culture conditions. ASCs derived from WAT were successfully differentiated in 3D poly(ethylene glycol) hydrogels into mature adipocytes with BAT phenotype and function, including high uncoupling protein 1 (*UCP1*) mRNA and protein expression and increased metabolic activity (basal oxygen consumption, proton leak, and maximum respiration). By utilizing this ''browning'' process, the abundant and accessible WAT stem cell population can be engineered into 3D tissue constructs with the metabolic capacity of native BAT, ultimately for therapeutic intervention *in vivo* and as a tool for studying BAT and its metabolic properties.

Keywords: adipose-derived stem cells, brown adipose tissue, 3D hydrogels, adipogenesis, metabolic profiling, oxygen consumption rate

Introduction

Engineered adipose tissue is used to study metabolism and drug responses and can be used for reconstruction of soft tissue lost due to trauma, disease, or congenital abnormalities.[1] Tissue engineering efforts have focused on white adipose tissue (WAT): the type of body fat that serves primarily as an energy storage organ, yet also fulfills many crucial endocrine functions.[2] Because excess WAT is a hallmark of obesity and its physiological sequelae, it is often considered an Achilles heel of the Western world. If current trends prevail, the United States Centers for Disease Control and Prevention report that up to one-third of Americans will have type 2 diabetes resulting from obesity by 2050.[3] Other developed and developing nations face similar obesity challenges, representing an enormous imminent burden on healthcare and millions of patients worldwide.

To combat this pressing issue, another type of adipose tissue has been identified as a potential weapon in counteracting the negative metabolic consequences associated with obesity.[4] Brown adipose tissue (BAT) is morphologically different from WAT, with smaller cells featuring increased amounts of associated extracellular matrix, numerous smaller lipid vacuoles, and a distinct brown color owing to higher mitochondrial content.[5] BAT functions quite differently than WAT, since brown adipocytes have a higher metabolic activity characterized by the process of mitochondrial uncoupling. Uncoupling protein 1 (UCP1) is highly expressed in the mitochondria of brown adipocytes and mediates their unique metabolic function through the uncoupling of ATP production from oxygen consumption in the electron transport chain (ETC). Mitochondrial uncoupling leads to futile cycling of ATP synthase, consuming oxygen, expending calories, and producing heat.[6]

Due to its role in nonshivering thermogenesis, BAT was previously considered relevant solely for thermoregulation

Translational Tissue Engineering Center and Departments of [1]Biomedical Engineering and [2]Cellular and Molecular Medicine, Johns Hopkins University, Baltimore, Maryland.
[3]Department of Biology, Ecole Polytechnique, Palaiseau, France.
[4]Department of Biomedical Engineering and High-Throughput Biology Center, Johns Hopkins University, Baltimore, Maryland.
*These two authors contributed equally to this work.

in hibernating mammals and in human infants. However, the presence of active BAT in adult humans has recently been documented in multiple anatomical locations, including the supraclavicular region, subcutaneous regions near the neck, as well as other visceral regions near large blood vessels and organs.[7] The quantity of BAT in adult humans appears to correlate inversely with body mass index, indicating an expanded role for BAT in metabolic and energy homeostasis.[8]

In mouse studies, transplantation of BAT completely reversed high-fat diet-induced insulin resistance, decreased total body fat mass, and improved glucose tolerance and insulin sensitivity.[9] Similar metabolic benefits have been observed with BAT transplantation into leptin-deficient ob/ob mice and with activation of native BAT by cold exposure in humans.[10,11] Researchers estimate that only two ounces of BAT can burn up to 500 calories per day, implying significant therapeutic potential to treat obesity and related diseases and making BAT an ideal target for tissue engineering.[12]

The precursors of native BAT are the multipotent mesenchymal stem cells found in adipose tissues, otherwise known as adipose-derived stem cells (ASCs). Previous work in the field has identified two different types of brown adipocytes with distinct developmental lineages. Classical brown adipocytes typical of interscapular BAT depots originate from myogenic factor 5 (Myf5)-positive muscle precursor cells, whereas inducible brown adipocytes found scattered in WAT come from a Myf5-negative lineage, yet possess many of the same characteristics of classical brown adipocytes.[13] Because native BAT reservoirs are minimal, methods for converting an existing, abundant source of precursor cells are needed to leverage the capacity of BAT to regulate metabolic function. The ASCs present in WAT (wASCs) that are able to differentiate toward a brown adipocyte phenotype are an ideal source material for generating engineered BAT.[12]

To engineer BAT, we isolated ASCs from rodent brown interscapular fat and rodent and human white subcutaneous adipose depots, and then induced adipocyte differentiation in two-dimensional (2D) monolayer culture and in three-dimensional (3D) hydrogels. Differentiation was accomplished using standard adipogenic media that contain specific agents previously shown to trigger either white or brown adipogenesis.[14,15] Mature adipocytes generated from wASCs in browning conditions exhibited an increased metabolic activity compared to wASC-derived white adipocytes, indicating a successful transition of WAT-derived progenitors into functionally brown adipocytes in 2D and 3D culture. Our strategy allows for metabolic characterization of different preadipocyte populations and evaluation of their brown adipogenic differentiation potential with different biomaterials that can mimic the 3D tissue environment and support mature tissue formation.

Materials and Methods

ASC isolation

Rat ASCs were isolated from the subcutaneous WAT (wASCs) and interscapular BAT depots (bASCs) of female Sprague-Dawley rats. Human wASCs were isolated from subcutaneous WAT obtained from a single patient undergoing an abdominoplasty procedure. ASCs were separated by digestion of the whole tissue with 1 mg/mL collagenase I (Worthington) in Dulbecco's Modified Eagle Medium-F12 (DMEM-F12; Invitrogen) for 1.5 h on an orbital shaker at 37°C. The cell suspension was centrifuged and erythrocytes were lysed with a solution of 155 mM NH_4Cl, 10 mM $KHCO_3$, and 0.1 mM ethylenediaminetetraaceticacid, adjusted to pH 7.3, and the slurry was passed through a 40 μm cell strainer and centrifuged. The ASC pellet was resuspended and seeded at 5000 cells/cm^2 on polystyrene tissue culture plates in basic growth media: DMEM-F12 (Invitrogen), 10% fetal bovine serum (FBS; Thermo Fisher Scientific), and 1% PenStrep (Invitrogen). For human ASCs, 1 ng/mL of basic fibroblast growth factor was included in the growth media to stimulate cell growth. Cell passage number was kept consistent for all studies between 5 and 7.

2D adipogenesis

ASCs were differentiated in standard 2D monolayer culture for 4 weeks before histological analysis and for 1, 2, 3, and 4 weeks for gene expression analysis. For metabolic analysis, 4-week cultures were replated and maintained in differentiation media for an additional 1 week in Seahorse XF24 islet capture microplates coated in 0.1% gelatin (20,000 cells/well). Rat and human wASCs were differentiated in white and brown adipogenic conditions; rat bASCs were only differentiated in the brown adipogenic medium (Fig. 1).

For all experiments, ASCs were seeded in six-well polystyrene tissue culture plates at a density of 12,000 cells/cm^2. The white adipogenic differentiation medium contained the following: 1 μM dexamethasone, 200 μM indomethacin, 500 μM 3-isobutyl-1-methylxanthine (IBMX), 10 μg/mL bovine insulin, 1% PenStrep (Invitrogen), and 10% FBS (Thermo Fisher Scientific) in high-glucose DMEM (Invitrogen).[15] The brown adipogenic differentiation medium contained the following: 0.5 μM dexamethasone, 125 nM indomethacin, 250 μM IBMX, 850 nM bovine insulin, 1 μM rosiglitazone (Cayman Chemical), 1 nM triiodothyronine (T3), 1% PenStrep (Invitrogen), and 10% FBS (Thermo Fisher Scientific) in high-glucose DMEM (Invitrogen).[14] The brown adipogenic differentiation medium for human ASCs contained a higher T3 concentration of 120 nM, which was optimized to achieve a comparable level of differentiation to that observed in rat cells. Unless otherwise noted, reagents were obtained from Sigma-Aldrich.

3D adipogenesis

Poly(ethylene glycol)-diacrylate (PEGDA, MW 3.4 kDa) hydrogels were formed by mixing 5% w/v PEGDA in sterile phosphate-buffered saline (PBS, pH 7.4) with 0.05% w/v Irgacure 2959 (Ciba). ASCs were homogenously suspended in the hydrogel solution (2×10^4 cells/μL); the solution was then transferred immediately into Seahorse XF24 islet capture screen inserts, which served as a cylindrical mold (5 mm diameter × 1 mm height). Hydrogel constructs (20 μL) were cross-linked by UV exposure for 5 min to achieve gelation. ASCs were cultured in the adipogenic medium for 4 weeks before histological and gene expression analysis. For metabolic analysis of 3D constructs, hydrogels were transferred to a 24-well Seahorse XF islet capture microplate after 4 weeks in differentiation media and then maintained in differentiation media for an additional 1 week. Unless otherwise noted, reagents were obtained from Sigma-Aldrich.

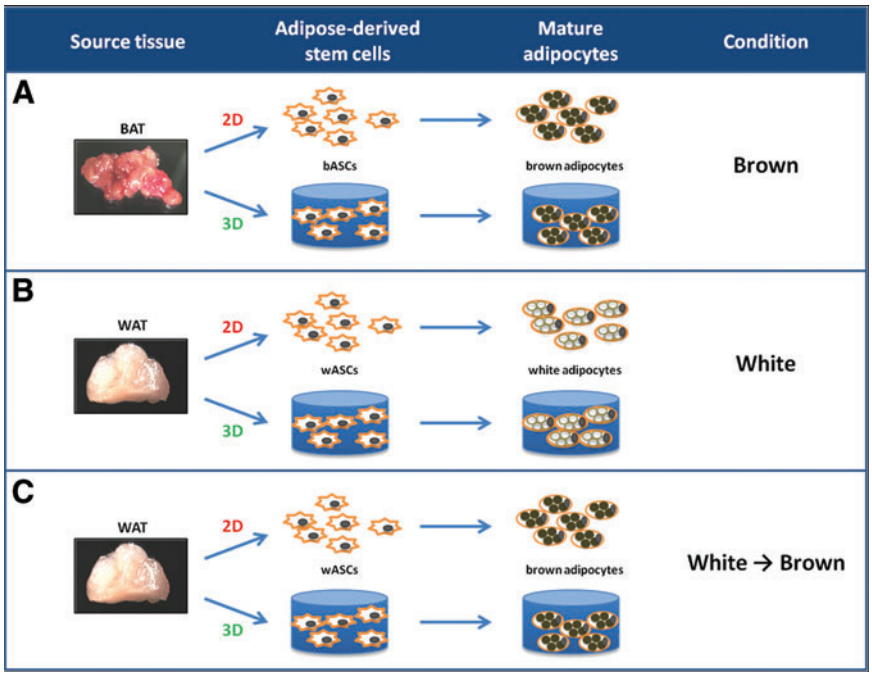

FIG. 1. Tissue culture methods. **(A)** ASCs isolated from rat BAT (bASCs) are cultured in brown adipogenic medium as a monolayer and encapsulated in 5% PEG hydrogels to produce mature brown adipocytes. **(B)** ASCs isolated from rat and human WAT (wASCs) are cultured in white adipogenic medium in the same 2D and 3D conditions to produce mature *white* adipocytes. **(C)** ASCs derived from rat and human WAT (wASCs) undergo browning in brown adipogenic medium, producing mature adipocytes with the phenotype and metabolic function of BAT. BAT, brown adipose tissue; ASC, adipose-derived stem cells; bASC, ASC isolated from rat BAT; PEG, poly(ethylene glycol); wASC, ASC isolated from either rat or human WAT; WAT, white adipose tissue. Color images available online at www.liebertpub.com/tea

Histological analysis

For 2D cultures, cell monolayers were fixed in 10% formalin for 30 min before staining. Rabbit anti-peroxisome proliferator-activated receptor gamma (PPARγ) antibody (Santa Cruz Biotechnology) and anti-UCP1 antibody (Abcam) were applied in titers of 1:50 and 1:500, respectively, and then incubated overnight at 4°C followed by incubation with Alexa Fluor 594-conjugated goat anti-rabbit immunoglobulin G (H + L) secondary antibody (Life Technologies) for visualization. The nuclei were stained with Hoechst 33342 dye (Invitrogen). Adipocytes were also stained with Oil Red O solution (3 mg/mL in 50.4% triethyl phosphate) to assess intracellular lipids.

For immunohistochemistry of 3D cultures, constructs were fixed, paraffinized, and sectioned using standard dehydration and embedding procedures to obtain 5 μm sections. Antigen retrieval was performed by immersing the slides in a citrate buffer and heating in a humidified chamber for 30 min, followed by blocking with 1% bovine serum albumin and 1% Tween-20 in PBS for 1 h. The antibodies were incubated as in 2D, followed by endogenous peroxidase quenching in a methanol and hydrogen peroxide solution. The primary antibodies were detected using horseradish peroxidase polymer-conjugated anti-rabbit secondary antibody (SuperPicture Polymer Detection Kit DAB; Life Technologies). For Oil Red O staining of hydrogel constructs, 10 μm frozen sections were obtained by sequential infiltration of constructs with graded sucrose-PBS solutions and optimum cutting temperature compound (Tissue-Tek) before cryosectioning. Unless otherwise noted, reagents were obtained from Sigma-Aldrich.

Real-time RT-polymerase chain reaction

Expression of canonical BAT and WAT markers were followed during the differentiation of the precursor cells into white and brown adipose lineages. Relative gene expression was quantified in 2D conditions on day 0, 7, 14, 21, and 28; 3D conditions were assayed on day 28 only ($n = 3$). General adipose differentiation markers (present in both WAT and BAT) included the following: adiponectin (*ADIPOQ*), an endocrine hormone secreted almost exclusively from adipose tissue that modulates glucose regulation and fatty acid oxidation[1]; transcription factor *PPARγ*, a master regulator of adipose tissue controlling pathways that stimulate lipid uptake, activate fatty acid storage, regulate glucose metabolism, and trigger adipogenesis[16]; and fatty acid binding protein 4 (*FABP4*), a key chaperone protein for fatty acid uptake into adipocytes.[1] Brown adipose markers were *UCP1* and cell death-inducing DFFA-like effector A (*CIDEA*). As a canonical BAT marker, *UCP1* facilitates the thermogenic properties of BAT by disrupting the mitochondrial proton gradient formed during oxidative phosphorylation, thereby uncoupling energy expenditure from ATP production.[5] *CIDEA* is also found predominantly in BAT and has been shown to regulate *UCP1*.[17]

RNA extraction was carried out with Trizol reagent (Invitrogen) according to the manufacturer information, including the addition of 1 μg of glycogen to each sample to aid in RNA precipitation. Reverse transcription was performed using the SuperScript RT III kit (Invitrogen) according to the manufacturer's instructions. Real-time reverse transcriptase-polymerase chain reaction (RT-PCR) was carried out with Power SYBR Green Master Mix (Life Technologies) on a StepOne Plus system (Applied Biosystems). Relative quantitation was performed using the ΔΔCt method with β-actin as the housekeeping gene for all conditions. Primer sequences are listed in Table 1.

In 2D time course studies, data are normalized to the earliest time point for each condition (Figs. 2D, E and 3D, E). For 3D studies, data are normalized to the ''White'' condition at the experimental endpoint of 4 weeks (Figs. 2I and 3I). When calculating ratios between 3D and 2D gene expression, the 2D and 3D relative quantification values

TABLE 1. REAL-TIME RT-PCR PRIMER SEQUENCES

Species	*Gene*	*Forward Sequence 5′-3′*	*Reverse sequence 5′-3′*
Rat	*Adipoq*	TGGTCCCTCCACCCAAGGAAA	ACACCTGCGTCTCCCTTCTCT
	Pparγ	TCAAAAGCCTGCGGAAGCCC	TGGGCGGTCTCCACTGAGAATAA
	Fabp4	GCCTTTGTGGGGACCTGGAAA	GCGAAGCCAACTCCCACTTCTT
	Ucp1	TGGTGAGTTCGACAACTTCC	GTGGGCTGCCCAATGAATAC
	Cidea	TGGAAAAGGGACAGAAATGG	TCTTCTGTGTCACCCAGTGC
	β-actin	CGGTCAGGTCATCACTATCGGCA	GCCACAGGATTCCATACCCAGGA
Human	*ADIPOQ*	CTG TTG CTG GGA GCT GTT CT	CCCTTAGGACCAATAAGACCTGG
	PPARγ	AGGAGAAGCTGTTGGCGGAGA	TGCTTTGGTCAGCGGGAAGG
	FABP4	ACAGGAAAGTCAAGAGCACCATAACC	TGACGCATTCCACCACCAGTTT
	UCP1	TCCAGGTCCAAGGTGAATGC	ACTAGGTGCTGTTTCTTTCCCT
	CIDEA	TAAGCGAGTCCTGTTCACCC	GCATCCAGAGTCTTGCTGATG
	β-ACTIN	GGCACCCAGCACAATGAA	GCTAACAGTCCGCCTAGAAGC

ADIPOQ, adiponectin; *CIDEA*, cell death-inducing DFFA-like effector A; *PPARγ*, peroxisome proliferator-activated receptor gamma; *FABP4*, fatty acid binding protein 4; *UCP1*, uncoupling protein 1; RT-PCR, reverse transcriptase-polymerase chain reaction.

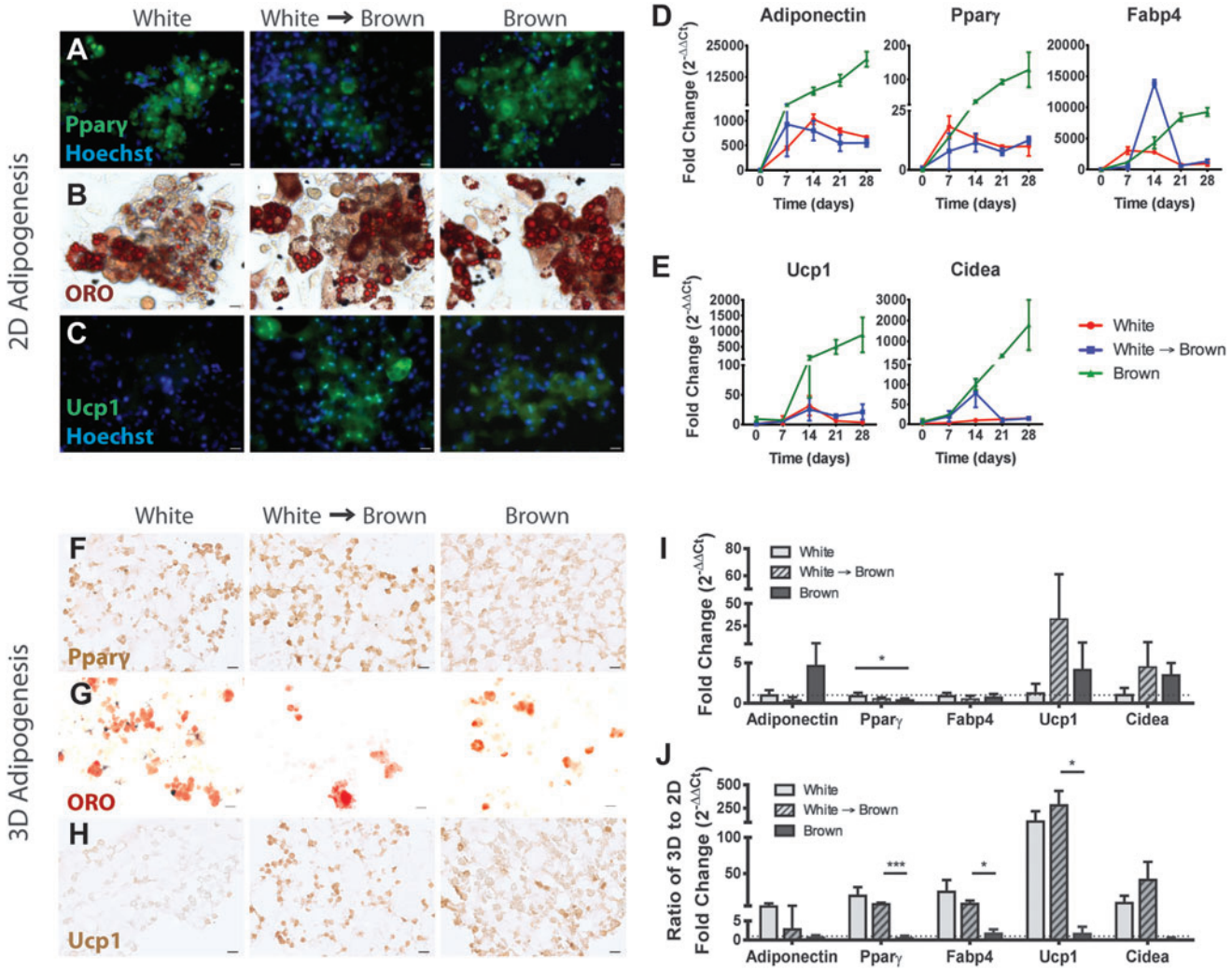

FIG. 2. Differentiation of rat wASCs and bASCs. **(A)** PPARγ, **(B)** UCP1 immunostaining, and **(C)** Oil Red O staining after 4 weeks of 2D *in vitro* culture. Hoechst dye represents nuclear staining. **(D)** Time course of 2D gene expression for white adipose markers and **(E)** brown adipose markers over 4 weeks, normalized to white adipocyte expression on day 0. **(F)** PPARγ, **(G)** UCP1 immunostaining, and **(H)** Oil Red O staining after 4 weeks of 3D *in vitro* encapsulation in 5% PEG hydrogels. **(I)** Gene expression in 3D constructs at 4 weeks, normalized to expression in the ''White'' condition. **(J)** Ratio of gene expression in 3D-cultured versus 2D-cultured populations at 4 weeks, each normalized to the 2D ''White'' condition on day 28 (4 weeks). *p*-Values < 0.05 were considered significant (*< 0.05, **< 0.005, ***< 0.0005). 2D, two dimensional; 3D, three dimensional; PPARγ, peroxisome proliferator-activated receptor gamma; UCP1, uncoupling protein 1. Color images available online at www.liebertpub.com/tea

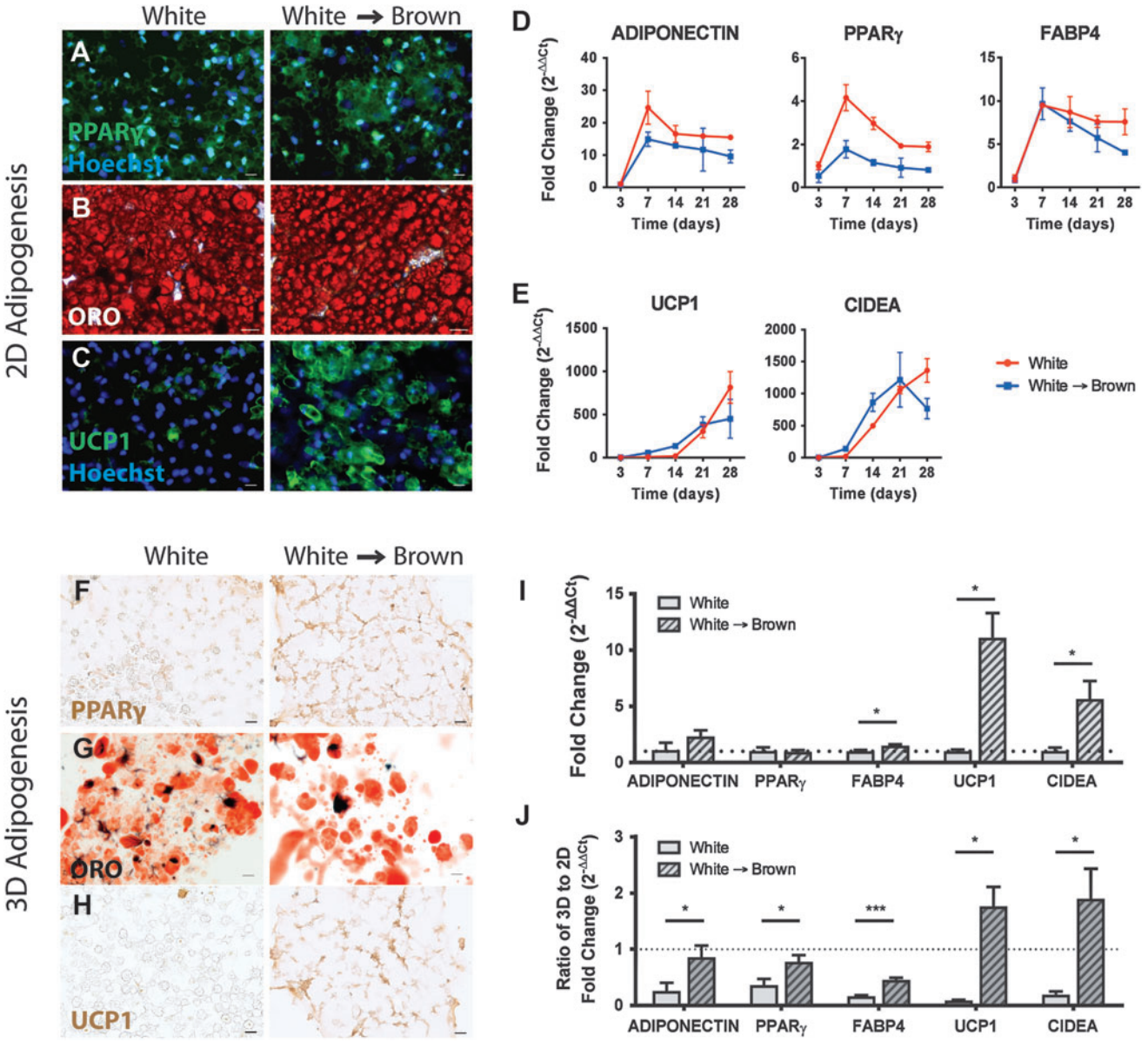

FIG. 3. Differentiation of human wASCs. **(A)** PPARγ, **(B)** UCP1 immunostaining, and **(C)** Oil Red O staining after 4 weeks of 2D *in vitro* culture. Hoechst dye represents nuclear staining. **(D)** Time course of 2D gene expression for white adipose markers and **(E)** brown adipose markers over 4 weeks, normalized to white adipocytes expression on day 0. **(F)** PPARγ, **(G)** UCP1 immunostaining, and **(H)** Oil Red O staining after 4 weeks of 3D *in vitro* encapsulation in 5% PEG hydrogels. **(I)** Gene expression in 3D constructs at 4 weeks, normalized to expression in the ''White'' condition. **(J)** Ratio of gene expression in 3D-cultured versus 2D-cultured populations at 4 weeks, each normalized to the 2D ''White'' condition on day 28 (4 weeks). *p*-Values < 0.05 were considered significant (*< 0.05, **< 0.005, ***< 0.0005). Color images available online at www.liebertpub.com/tea

were first determined by normalizing to the 2D ''White'' condition at the experimental endpoint of 28 days (4 weeks).

RNA sequencing

RNA sequencing was performed at the Johns Hopkins Deep Sequencing and Microarray Core. The sequencing library was constructed using a paired end, 75 bp pair run on a HiSeq Illumina sequencing platform and the rn4 index for *Rattus norvegicus* as a reference genome. HTseq was used to obtain the raw read counts and DESeq was run to test for differential expression.[18,19] Genes were considered differentially expressed if they surpassed a threshold set at 5% family-wise error rate (0.05/number of genes having read counts greater than zero).

Metabolic analysis

A mitochondrial stress test was performed to analyze cellular metabolic activity of the differentiated cell populations ($n = 5$) using a Seahorse XF24 Flux Analyzer (Seahorse Bioscience). The XF Analyzer measures the oxygen consumption rate (OCR) of live cells in real time and utilizes sequential application of drugs that inhibit different enzymes in the ETC to determine metabolic parameters such as basal and maximal cellular respiration, proton leak, and spare capacity.[20]

After the initial OCR reading, oligomycin is applied to inhibit ATP synthase, removing the portion of the OCR contributed by ATP production and revealing proton leak in the ETC (after correcting for nonmitochondrial oxygen consumption). Second, the ionophore carbonyl cyanide-*p*-trifluoromethoxyphenylhydrazone (FCCP) is applied to induce maximum respiration by collapsing the inner membrane potential and leading to rapid consumption of oxygen without the generation of ATP. Finally, rotenone and antimycin A are used to inhibit the ETC enzymes upstream of oxygen consumption, thus eliminating all mitochondrial oxygen expenditure. The final OCR represents the background nonmitochondrial oxygen consumption of the cells. Subtracting the final OCR after rotenone/antimycin A treatment from initial OCR before oligomycin treatment gives the mitochondrial basal metabolism or the mitochondrial OCR at resting state.[21]

For the 2D studies, cells were placed in a 37°C incubator without CO_2 for 45 min before the assay. After basal measurements, oligomycin (1 μM), FCCP (250 nM), and rotenone/antimycin A (2 μM/2 μM) were injected sequentially to characterize the mitochondrial function of the cells. At least four measurements were taken before and following the application of each drug solution. Oligomycin, FCCP, and rotenone/antimycin A were injected into the medium at 84, 136, and 170 min, respectively, in rat 2D experiments. Human 2D injections times were 85, 120, and 154 min, respectively.

To analyze cellular respiration in hydrogel-encapsulated cells, the same drug concentrations were used as for the 2D mitochondrial stress test, but injection times were increased to allow for diffusion within the constructs. Drugs were injected in rat 3D experiments at 97, 207, and 317 min, respectively; similarly, human 3D injections occurred at 82, 192, and 261 min.

PicoGreen DNA quantification assays were performed to normalize the OCR measurements. Basal metabolic rate, proton leak, and maximal respiration were recorded for all conditions.

Statistical analysis

All results are expressed as arithmetic mean with error bars representing ±1 standard deviation from the mean. For gene expression studies, three biological replicates ($n=3$) were analyzed for each condition and time point; for the metabolic studies, five biological replicates per condition ($n=5$) were analyzed. Student's *t*-tests and one-way analysis of variance with Tukey's post-test were conducted with GraphPad Prism software. *p*-Values <0.05 were considered significant (*<0.05, **<0.005, ***<0.0005).

Results

White and brown adipogenesis of rat ASCs in 2D monolayer culture

Rat wASC and bASC populations were morphologically indistinguishable yet distinct in their gene expression profiles before differentiation. Although *Ucp1* and *Cidea* are associated with mature BAT, both genes were more highly expressed in bASCs, while the canonical adipose genes *Adiponectin*, *Pparγ*, and *Fabp4* were more highly expressed in wASCs (Supplementary Fig. S1; Supplementary Data are available online at www.liebertpub.com/tea).

Rat and human wASCs were differentiated in white and brown adipogenic conditions; rat bASCs were only differentiated in the brown adipogenic medium (Fig. 1). After 4 weeks of culture in white or brown adipogenic medium, each type of ASC produced mature adipocytes, as evidenced by positive staining for PPARγ (Fig. 2A) and the presence of intracellular lipid droplets (Fig. 2B). Most critically, wASCs and bASCs grown in brown conditions both produced UCP1-expressing adipocytes, indicating that a brown phenotype can be induced in stem cells from a white adipose lineage (Fig. 2C).

Expression of adipocyte genes increased for all three experimental conditions, indicating successful differentiation. Differentiation of wASCs in either white or brown media resulted in earlier peak expression of *Adiponectin*, *Pparγ*, and *Fabp4* between day 7 and day 14, whereas expression of these genes trended upward throughout the study in bASCs differentiated in the brown medium (Fig. 2D). Expression of the mature BAT markers *Ucp1* and *Cidea* increased in the bASC-derived brown adipocyte population, as expected, and peaked in the wASC-derived brown adipocyte population by day 14 (Fig. 2E). In general, the bASCs had greater relative changes in gene expression between day 0 and 28 than either of the wASC populations.

Additional characterization was performed on rat adipocytes differentiated in 2D to identify key differences in the gene expression profiles between wASC-derived white adipocytes and bASC-derived brown adipocytes. RNA sequencing analysis identified 44 genes that are differentially expressed at significant levels between these two groups (Supplementary Fig. S2). Fifteen of the forty-four differentially expressed genes were directly involved in cellular metabolism, and all fifteen metabolic genes were more highly expressed in the brown adipocytes (Supplementary Fig. S2C). Eight of the metabolic genes were validated by RT-PCR with comparable results to RNA sequencing (Supplementary Fig. S2A, B).

White and brown adipogenesis of rat ASCs in 3D

To produce 3D BAT constructs, rat wASCs and bASCs were seeded inside 5% PEG hydrogels using techniques previously optimized for promoting adipogenesis.[22] wASCs and bASCs were cultured to undergo brown adipogenesis; white adipogenesis of wASCs served as a control (Fig. 1). Following 4 weeks of *in vitro* culture in differentiation media, each of the three cell populations displayed strong adipogenesis by positive PPARγ and Oil Red O staining (Fig. 2F, G). Cells cultured in brown adipogenic conditions expressed UCP1 ubiquitously, whereas the wASCs cultured in white adipogenic conditions expressed little UCP1 (Fig. 2H). These histological results corresponded with gene expression at 4 weeks (Fig. 2I). Both brown adipogenic populations demonstrated increased expression of *Ucp1* and *Cidea* compared to the white adipocytes, with eight-fold higher *Ucp1* expression in wASC-derived brown adipocytes than in bASC-derived brown adipocytes. The wASCs cultured in brown adipogenic conditions expressed *Cidea* comparable to bASCs in similar conditions (Fig. 2I).

Adipose gene expression in 3D and 2D conditions was compared at 4 weeks (Fig. 2J). Gene expression in the bASC-derived population was similar between 2D and 3D conditions. However, for wASC-derived populations, gene expression was

significantly higher in the 3D hydrogels than in 2D culture, indicating possible favorability of the PEG hydrogels for wASC differentiation. For wASC-derived brown adipocytes in particular, the 3D environment enhanced *Ucp1* expression relative to 2D. A similar trend held for *Cidea* expression, although *Cidea* expression was slightly decreased in the bASC-derived brown adipocyte 3D constructs relative to 2D culture (Fig. 2J). Since the differentiated bASCs had much lower 3D to 2D ratios than wASCs for all markers, this suggests that the bASCs perform relatively poorly in a 3D environment. Unmet oxygen or nutrient demands in these highly metabolically active stem cells may account for the differences of 3D culture favorability between bASCs and wASCs.

Browning of human wASCs in 2D monolayer culture

Human wASCs were isolated from abdominoplasty discards to validate the potential of inducing brown adipogenic differentiation in human cells. After 4 weeks in 2D culture, the human wASCs differentiated toward an adipogenic lineage with strong PPARγ expression and presence of intracellular lipids (Fig. 3A, B). wASCs differentiated toward a brown lineage stained more robustly for UCP1 protein than white adipocytes (Fig. 3C). Similar to rat 2D cultures, expression of characteristic adipose genes *Adiponectin*, *PPARγ*, and *FABP4* in differentiated human wASCs peaked on day 7 and was relatively higher in white adipocytes than wASC-derived brown adipocytes (Fig. 3D). Stimulation with the brown adipogenic medium increased *UCP1* expression several hundredfold relative to the undifferentiated wASCs, indicating a functional difference between the wASC progenitors and mature brown adipocytes.

Unlike the corresponding rat 2D culture, the human white adipocyte population had higher peak expression of *UCP1* than the wASC-derived brown adipocytes on day 28, although this difference was not significant (Fig. 3E), indicating that unintended ''browning'' occurred in the white adipogenic condition. In both conditions, brown adipose gene expression increased enormously relative to the earliest time point.

Browning of human wASCs in 3D

After 4 weeks of 3D culture, both human wASC-derived populations underwent adipogenesis (Fig. 3F, G), with no significant difference between the two conditions in the expression of white adipogenic markers *Adiponectin*, *PPARγ*, and *FABP4* (Fig. 3I). Brown adipocytes expressed significantly higher levels of brown adipogenic markers *UCP1* and *CIDEA* compared to white adipocytes (Fig. 3I), also reflected by stronger UCP1 staining (Fig. 3H). Expression of all genes was higher in 2D than 3D for white adipocytes. Similar to rat cells, human wASC-derived brown adipocytes increased expression of both brown adipose markers in 3D over the 2D condition, indicating that the 3D condition enhances brown adipogenic differentiation for human wASCs (Fig. 3J).

Metabolic function of rat and human ASCs in vitro

The unique metabolic profile of brown adipose is a defining feature and correlates with therapeutic relevance to diabetes and obesity. As measurements of cellular metabolic activity, we quantified OCR of mature human wASC-derived and rat wASC- and bASC-derived white and brown adipocytes after 5 weeks in 2D or 3D *in vitro* culture. Mitochondrial basal metabolism, proton leak (mitochondrial uncoupling, a key characteristic of brown adipocytes), and maximum respiration were elucidated by sequential application of drugs that target components of the ETC and other mitochondrial structures. Mature brown adipocytes were expected to have a greater basal metabolism, proton leak, and maximal respiration compared to white adipocytes.[21,23]

OCR was measured while applying oligomycin (ATP synthase inhibitor), FCCP (induces maximal respiration), and rotenone/antimycin A (inhibit ETC enzymes upstream of oxygen consumption), in succession over the course of several hours (Fig. 4A). In 2D culture, the basal respiration, proton leak, and maximum respiration of both the rat wASC- and bASC-derived brown adipocytes were significantly higher than in white adipocytes (Fig. 4B). This functional result is consistent with the observed increase in UCP1, as energy expenditure is expected to increase as a result of mitochondrial uncoupling (Fig. 2C, E). Both wASC- and bASC-derived brown adipocytes demonstrated higher maximal respiration than white adipocytes, with the bASC-derived population exhibiting the greatest maximal respiration (Fig. 4B). Similar trends were apparent in 3D culture of rat adipocytes; however, for basal respiration and proton leak, variability in the wASC-derived brown adipocyte population was too great to show a significant difference from the white adipocytes (Fig. 4C).

For human adipocytes in 2D, the white adipocytes and wASC-derived brown adipocytes had a comparable metabolic activity with no significant differences in basal metabolism, proton leak, or maximal respiration (Fig. 4D). This result corresponds to the 2D gene expression data, which also indicate that unintended browning may have occurred in the highly confluent 2D wASC-derived white adipocyte population. In 3D, however, the wASC-derived brown adipocytes were more metabolically active by all measures (Fig. 4E), indicating the favorability for human WAT progenitors for engineering function BAT.

Discussion

In recent years, brown fat has become increasingly attractive as a therapeutic target for obesity and diabetes. Several pharmacological and transplantation approaches have been considered to convert or activate existing adipose to increase energy expenditure, but long-term success is limited due to the safety profiles of pharmacological agents and the limited supply of transplantation sources.[12] Since browning agents generally target highly conserved pathways, systemic dosing of ''browning'' agents can produce dangerous off-target side effects. Local delivery of induced brown adipocytes may provide a safer alternative.

In this work, we successfully engineered metabolically active human brown adipose from white adipose progenitors and compared the brown differentiation potential of stem cell populations from human and rat adipose depots. Metabolic analysis demonstrated that brown adipocytes produced from wASCs by transdifferentiation sustained long-term metabolic output similar to the classical brown adipocytes derived from bASCs. In addition, rat wASCs performed equally well or better than bASCs for engineering brown adipocytes with respect to expression of *Ucp1*, basal respiration, and proton leak in 3D hydrogels,

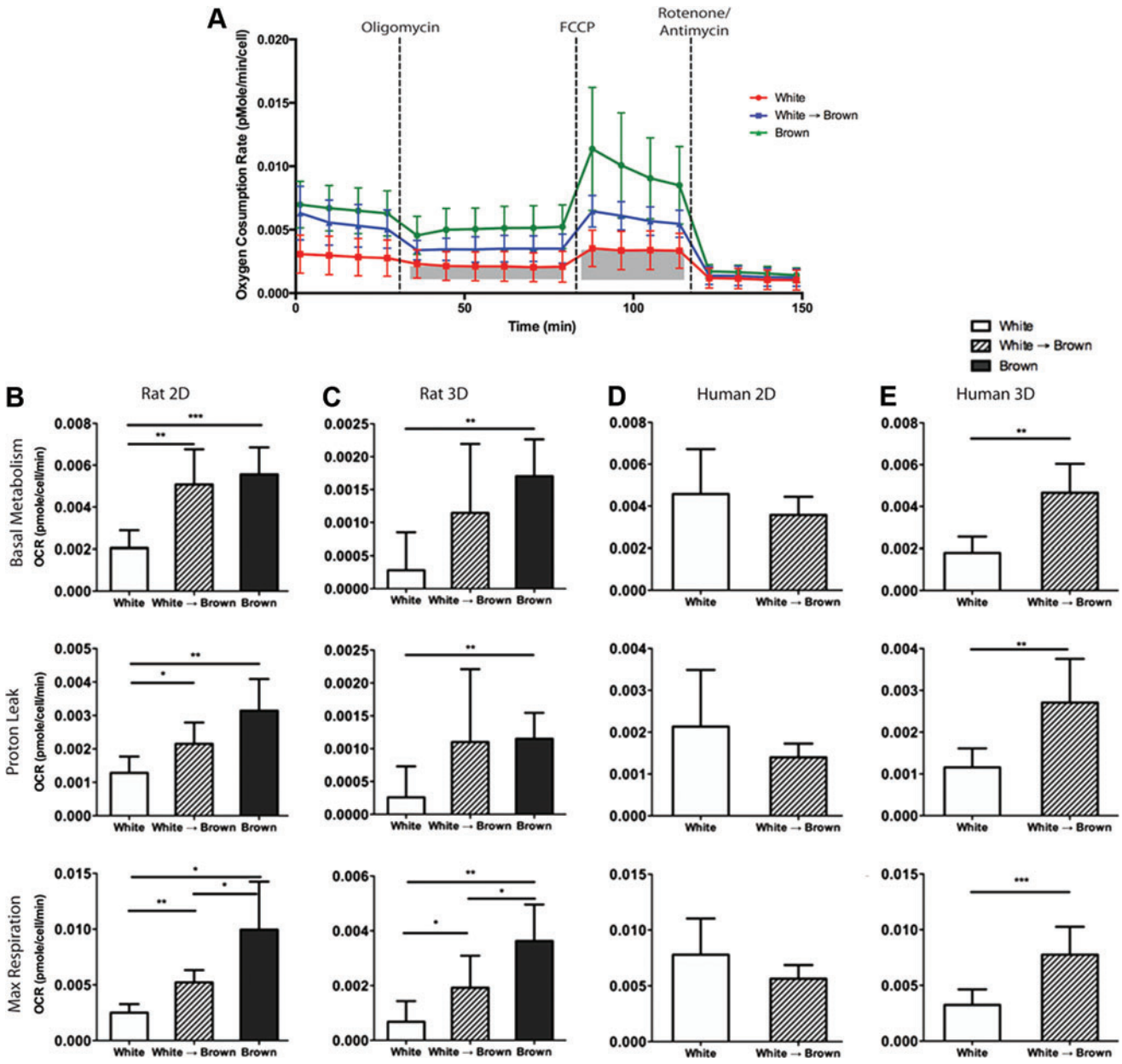

FIG. 4. Metabolic function of adipocytes in 2D and 3D culture. **(A)** Representative OCR plot of mitochondrial stress test for rat adipocytes in 2D culture. *Gray boxes* indicate the values for proton leak (*left*) and maximal respiration (*right*). OCR measurements after 5 weeks in adipogenic culture conditions for **(B)** rat adipocytes in 2D cultures, **(C)** rat adipocytes in 3D cultures, **(D)** human adipocytes in 2D cultures, and **(E)** human adipocytes in 3D cultures. *p*-Values < 0.05 were considered significant (*< 0.05, **< 0.005, ***< 0.0005). OCR, oxygen consumption rate. Color images available online at www.liebertpub.com/tea

underscoring the potential for wASCs as a building material for BAT in 3D environments.

In 2D, gene expression over time revealed dynamic differences between wASC and bASC differentiation. Rat wASCs reached a plateau in gene expression between 7 and 14 days, which may have been related to contact inhibition and growth arrest at confluency and the completion of adipogenesis,[24] while gene expression in bASCs trended upward for the entire 28-day study. Although the differentiated adipocyte populations derived from wASCs had similar gene expression in 2D, metabolism was more dependent on the differentiation conditions than on the original stem cell source. As such, the metabolic profile of transdifferentiated brown adipocytes was more similar to the classical brown adipocytes than white adipocyte controls. In 2D cultures, the classical brown adipocytes achieved higher maximum oxygen consumption, but had similar basal respiration and proton leak as brown adipocytes derived from wASCs. Functionally, this indicates that classical brown adipocytes have more spare capacity than those derived from wASCs, but both mature brown adipocyte populations expend the same amount of energy at resting state and are equally capable of mitochondrial uncoupling, regardless of the stem cell source.

An unexpected result was obtained from the long-term 2D differentiation of human wASCs in the white adipogenic

medium. Unlike in rat monolayer cultures, these human wASCs appeared to undergo transdifferentiation in the absence of brown adipogenic medium, with *UCP1* and *CIDEA* expression from white adipogenic cultures surpassing expression in the brown adipogenic cultures by day 28. In addition, metabolic analysis indicated that the human wASC-derived 2D populations have elevated oxygen consumption relative to normal white adipocytes, closely matching the performance of both human and rat transdifferentiated brown adipocytes. An explanation for this unintended browning of the white adipogenic cultures could be the presence of autocrine or paracrine factors triggering adaptive thermogenesis. White adipocytes have been previously shown to express high levels of UCP1 in response to lactate accumulation as a mechanism to alleviate redox stress,[25] which may have been present in these highly confluent long-term cultures.

In 3D, wASCs from both humans and rats could be differentiated into brown adipocytes that expressed key BAT markers and were more metabolically active than white adipocytes; in fact, the rat wASCs transdifferentiated in 3D had significantly higher *Ucp1* expression than classical brown adipocytes. Functionally, both types of rat brown adipocytes had similar oxygen consumption. Human wASCs transdifferentiated in 3D were also significantly more metabolically active than normal white adipocytes by all metabolic measures, demonstrating the capacity of wASCs to produce functional brown adipocytes with high energy expenditure.

Comparison of gene expression between 2D and 3D conditions revealed other distinctions between these stem cell populations. Gene expression in rat bASCs was not significantly altered between the 2D and 3D conditions; however, wASCs of either species performed differently depending on the culture environment. Rat wASC-derived adipocytes underwent more significant adipogenesis in 3D than in 2D, while human wASCs were less adipogenic in 3D than in 2D. With respect to BAT gene expression, transdifferentiated brown adipocytes of either species responded more favorably to 3D encapsulation than 2D cultures. This result is significant because any tissue engineering or *in vivo* approach will necessarily involve 3D conditions; therefore, the favorability of a 3D environment for brown differentiation of wASCs is promising.

In the 3D hydrogels, increased cellular density or presence of a diffusion gradient may deprive the interior cells of oxygen and nutrients,[26,27] with varying effects between different types of adipocytes. We hypothesize that bASCs may underperform wASCs in the 3D environment due to the greater energy demand of these more metabolically active stem cells. Hypoxia is linked to mitochondrial loss and dysfunction in the BAT of obese mice, yet it may also stimulate ''browning'' of WAT through UCP1 recruitment.[28] Tolerance to hypoxic conditions is a favorable quality for engineered tissues, as cells often have limited blood supply following *in vivo* implantation. Our data indicate that wASCs are better suited to 3D culture than bASCs and other studies support the ability of white adipose progenitors to thrive in hypoxic environments and trigger neovascularization and immune-modulatory responses.[29,30]

Both human and rat brown adipocytes generated from wASCs showed sustained metabolic function typical of BAT for up to 5 weeks, particularly in 3D cultures, including the high basal respiration and high levels of mitochondrial uncoupling essential for BAT function *in vivo*. However, RNA sequencing of rat white adipocytes and bASC-derived brown adipocytes differentiated in 2D culture did not identify many of the canonical brown fat genes as differentially expressed, including *Ucp1*, *Cidea*, *Pgc1α*, *Prdm16*, and *Cox8b*. However, the analysis does reveal global upregulation in the metabolic transcriptome of BAT relative to WAT. BAT dominates the pool of differentially expressed metabolic genes, including mitochondrial, lipolytic, glycolytic, and ketogenic enzymes; insulin growth factor and fatty acid binding proteins; and proteins involved in oxidative phosphorylation, amino acid biosynthesis, nucleotide and cholesterol metabolism, and adipocyte development. Other work in the field has uncovered many additional important BAT markers.[31–37] These data illustrate that many factors should be considered in defining these two populations of cells and also underscore the importance of evaluating the metabolic function of engineered BAT in addition to genotype.

Overall, we have demonstrated the potential for engineering BAT from wASCs, constituting a powerful tool for understanding BAT function *in vitro* and the potential to ultimately harness BAT metabolic capacity to fight obesity and related diseases. Other recent studies have reported successful *in vitro* differentiation of human BAT-derived stem cells in 3D scaffolds and implantation *in vivo* with sustained brown marker expression, and improved body weight and glucose homeostasis in a high-fat diet-fed mouse model.[38] Investigation of alternate biomaterials that promote the transdifferentiation of wASCs into brown adipocytes will also benefit future *in vivo* applications.[22,39,40] Moreover, tissue engineering strategies provide the opportunity to combine permissive biomaterials and progenitors with drugs or biological factors that enhance their survival or differentiation, including many previously identified browning agents that are not suited to system administration.[41,42] A combination of biomaterial and cell-based approaches will surely be needed to achieve longevity of transplanted brown adipocytes *in vivo*.[43] An ideal therapeutic implant would not only maintain the brown phenotype of transplanted cells but also mobilize and promote brown adipogenesis in host ASCs.

Although harvesting BAT from humans for therapeutic use and engineering is not feasible, ASCs from white adipose are readily accessible and already used in many existing clinical applications.[1] As a future therapeutic intervention, autologous stem cells obtained from WAT may be used to engineer BAT constructs *ex vivo* for implantation back into the patient. This work demonstrates the feasibility of a tissue engineering strategy to combat obesity-related metabolic disorders.

Acknowledgments

This work was supported by grants from the National Institute of Arthritis and Musculoskeletal and Skin Diseases (NIAMS, R01AR054005) and the U.S. Department of Defense (W81XWH-11-2-0022).

Disclosure Statement

No competing financial interests exist.

References

1. Choi, J.H., *et al.* Adipose tissue engineering for soft tissue regeneration. Tissue Eng Part B Rev **16,** 413, 2010.

2. Balistreri, C.R., Caruso, C., and Candore, G. The role of adipose tissue and adipokines in obesity-related inflammatory diseases. Mediators Inflamm **2010,** 802078, 2010.
3. Boyle, J.P., *et al.* Projection of the year 2050 burden of diabetes in the US adult population: dynamic modeling of incidence, mortality, and prediabetes prevalence. Popul Health Metr **8,** 29, 2010.
4. Yoneshiro, T., *et al.* Recruited brown adipose tissue as an antiobesity agent in humans. J Clin Invest **123,** 3404, 2013.
5. Cannon, B., and Nedergaard, J. Brown adipose tissue: function and physiological significance. Physiol Rev **84,** 277, 2004.
6. Nicholls, D.G., and Locke, R.M. Thermogenic mechanisms in brown fat. Physiol Rev **64,** 1, 1984.
7. Sacks, H., and Symonds, M.E. Anatomical locations of human brown adipose tissue: functional relevance and implications in obesity and type 2 diabetes. Diabetes **62,** 1783, 2013.
8. Celi, F.S. Brown adipose tissue—when it pays to be inefficient. N Engl J Med **360,** 1553, 2009.
9. Stanford, K.I., *et al.* Brown adipose tissue regulates glucose homeostasis and insulin sensitivity. J Clin Invest **123,** 215, 2013.
10. Chondronikola, M., *et al.* Brown adipose tissue improves whole-body glucose homeostasis and insulin sensitivity in humans. Diabetes **63,** 4089, 2014.
11. Liu, X., *et al.* brown adipose tissue transplantation reverses obesity in ob/ob mice. Endocrinology **156,** 2461, 2015.
12. Tharp, K.M., and Stahl, A. Bioengineering beige adipose tissue therapeutics. Front Endocrinol (Lausanne) **6,** 164, 2015.
13. Wu, J., *et al.* Beige adipocytes are a distinct type of thermogenic fat cell in mouse and human. Cell **150,** 366, 2012.
14. Sun, L., *et al.* Mir193b-365 is essential for brown fat differentiation. Nat Cell Biol **13,** 958, 2011.
15. Lennon, D.P., and Caplan, A.I. Mesenchymal Stem Cells for Tissue Engineering, in Culture of Cells for Tissue Engineering. Hoboken, NJ: John Wiley & Sons, Inc., 2006, pp. 23–59.
16. Ohno, H., *et al.* PPARgamma agonists induce a white-to-brown fat conversion through stabilization of PRDM16 protein. Cell Metab **15,** 395, 2012.
17. Nordstrom, E.A., *et al.* A human-specific role of cell death-inducing DFFA (DNA fragmentation factor-alpha)-like effector A (CIDEA) in adipocyte lipolysis and obesity. Diabetes **54,** 1726, 2005.
18. Anders, S., Pyl, P.T., and Huber, W. HTSeq—a Python framework to work with high-throughput sequencing data. Bioinformatics **31,** 166, 2015.
19. Anders, S., and Huber, W. Differential expression analysis for sequence count data. Genome Biol **11,** R106, 2010.
20. Ferrick, D.A., Neilson, A., and Beeson, C. Advances in measuring cellular bioenergetics using extracellular flux. Drug Discov Today **13,** 268, 2008.
21. Dranka, B.P., *et al.* Assessing bioenergetic function in response to oxidative stress by metabolic profiling. Free Radic Biol Med **51,** 1621, 2011.
22. Singh, A., *et al.* Modular multifunctional poly(ethylene glycol) hydrogels for stem cell differentiation. Adv Funct Mater **23,** 575, 2013.
23. Bugge, A., Dib, L., and Collins, S. Measuring respiratory activity of adipocytes and adipose tissues in real time. Methods Enzymol **538,** 233, 2014.
24. Rosen, E.D., *et al.* Transcriptional regulation of adipogenesis. Genes Dev **14,** 1293, 2000.
25. Vergnes, L., and Reue, K. Adaptive thermogenesis in white adipose tissue: is lactate the new brown(ing)? Diabetes **63,** 3175, 2014.
26. Caló, E., and Khutoryanskiy, V.V. Biomedical applications of hydrogels: a review of patents and commercial products. Eur Polym J **65,** 252, 2015.
27. Wu, Y., Joseph, S., and Aluru, N.R. Effect of cross-linking on the diffusion of water, ions, and small molecules in hydrogels. J Phys Chem B **113,** 3512, 2009.
28. Trayhurn, P., and Alomar, S.Y. Oxygen deprivation and the cellular response to hypoxia in adipocytes—perspectives on white and brown adipose tissues in obesity. Front Endocrinol (Lausanne) **6,** 19, 2015.
29. Moyer, H.R., and Namnoum, J.D. Autologous fat transfer: the progenitor cell response to different recipient environments. Aesthet Surg J **34,** 932, 2014.
30. Eto, H., *et al.* Adipose injury-associated factors mitigate hypoxia in ischemic tissues through activation of adipose-derived stem/progenitor/stromal cells and induction of angiogenesis. Am J Pathol **178,** 2322, 2011.
31. Ussar, S., *et al.* ASC-1, PAT2, and P2RX5 are cell surface markers for white, beige, and brown adipocytes. Sci Transl Med **6,** 247ra103, 2014.
32. Thomas, C., Auwerx, J., and Schoonjans, K. Bile acids and the membrane bile acid receptor TGR5—connecting nutrition and metabolism. Thyroid **18,** 167, 2008.
33. Bostrom, P., *et al.* A PGC1-alpha-dependent myokine that drives brown-fat-like development of white fat and thermogenesis. Nature **481,** 463, 2012.
34. Kong, X., *et al.* IRF4 is a key thermogenic transcriptional partner of PGC-1alpha. Cell **158,** 69, 2014.
35. Cypess, A.M., *et al.* Insulin/IGF-I regulation of necdin and brown adipocyte differentiation via CREB- and FoxO1-associated pathways. Endocrinology **152,** 3680, 2011.
36. Tseng, Y.-H., *et al.* New role of bone morphogenetic protein 7 in brown adipogenesis and energy expenditure. Nature **454,** 1000, 2008.
37. Shinoda, K., *et al.* Genetic and functional characterization of clonally derived adult human brown adipocytes. Nat Med **21,** 389, 2015.
38. Silva, F.J., *et al.* Metabolically active human brown adipose tissue derived stem cells. Stem Cells **32,** 572, 2014.
39. Wu, I., *et al.* An injectable adipose matrix for soft-tissue reconstruction. Plast Reconstr Surg **129,** 1247, 2012.
40. Wu, I., *et al.* Design and Translation of an Adipose-Derived Soft Tissue Substitute. Baltimore, MD: Johns Hopkins University School of Medicine, 2014.
41. Komajda, M., *et al.* Heart failure events with rosiglitazone in type 2 diabetes: data from the RECORD clinical trial. Eur Heart J **31,** 824, 2010.
42. Villarroya, F., and Vidal-Puig, A. Beyond the sympathetic tone: the new brown fat activators. Cell Metab **17,** 638, 2013.
43. Tharp, K.M., *et al.* Matrix-assisted transplantation of functional beige adipose tissue. Diabetes **64,** 3713, 2015.

Address correspondence to:
Jennifer H. Elisseeff, PhD
400 North Broadway, Smith 5035
Baltimore, MD 21231

E-mail: jhe@jhu.edu

Received: September 29, 2016
Accepted: December 16, 2016
Online Publication Date: February 21, 2017